

Novel Network-Based Approaches for Studying Cognitive Dysfunction in Behavioural Neurology

H2020-MSCA-RISE-2016-734718

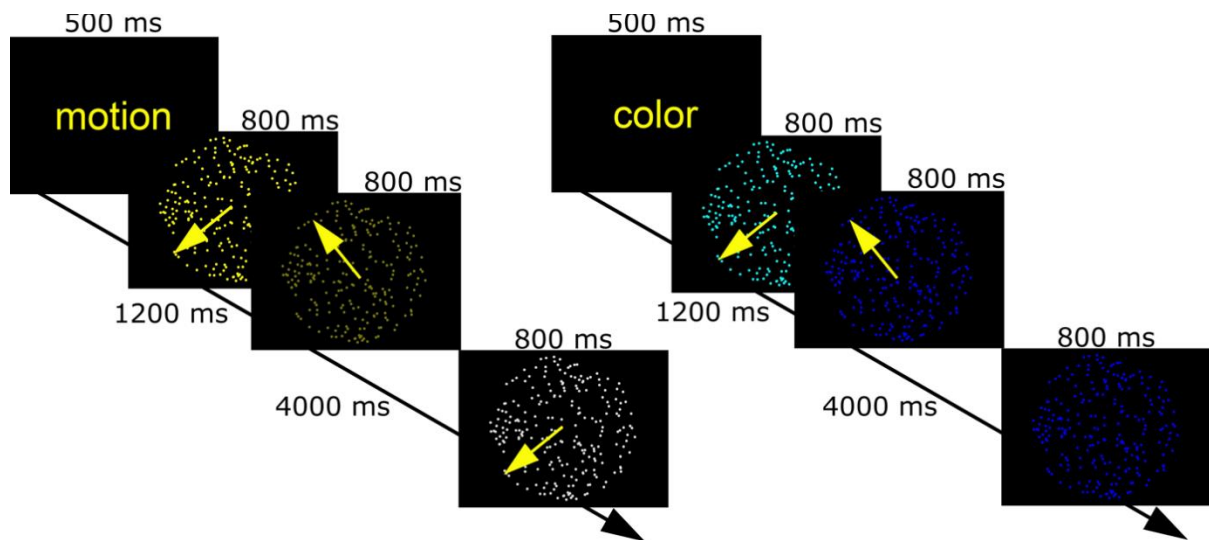


D4.5 Identification of alterations in patterns of brain activation and connectivity associated with deficient AMWM in PD using fMRI

Work Package:	WP4
Task:	-
Deliverable due date:	28.02.2022
Responsible partner:	USZ
Deliverable number:	D24
Deliverable type:	Report
Dissemination level:	PU

1 Task design

We employed a modified random dot kinematogram paradigm, in which participants attend a circular aperture containing coherently moving dots of a single color (Zanto & Gazzaley 2009). At the start of each trial, a text message appeared for 0.5 seconds, warning participants to attend a specific attribute of consequent stimuli (shade of colour or direction of motion). Afterwards, two consecutive random dot kinematograms were displayed for 0.8 seconds each, followed by a target stimulus after a rest period of 4 seconds. Participants had to decide whether the relevant attribute of the target was the same as it had been in one of the previous two kinematograms. Each trial lasted for 16.6 seconds, and there were 20 trials for each condition (40 altogether). For a depiction of the task, see Figure 1.



1.1 PARTICIPANTS

20 patients with PD and 20 healthy controls (HC) were recruited. 17 PD patients and 18 HC completed the study protocol, and 2 further PD and 2 HC were excluded due to extensive motion during the scans. 16 HC and 15 PD were included in the final analysis. Age and biological sex distribution did not differ significantly in the final analysed population (age - Student's independent samples T-test: $p > 0.05$; sex - Fisher's exact test: $p < 0.12$). All included participants were right-handed. All participants' eyesight was normal or corrected to normal and none of them reported difficulty performing the task. Healthy controls and PD patients were cognitively normal (MMSE-score ≥ 27 in all cases). Demographic data and clinical characteristics are described in Table 1.

	Healthy controls	Parkinson's disease
N	16	15
Age	64.63 +/- 8.84	65.34 +/- 6.81
Sex	8/9	11/4
UPDRSIII-motor	-	25.00 +/- 9.82
Hoehn-Yahr stage	-	3.0 (1-4)

Table 1. Demographic data of the participants.

1.2 IMAGE ACQUISITION

3D T1-weighted fast spoiled gradient echo images (FSPGR-IR, TR: 5.3 ms TE: 2.1 TI: 450 ms, slice thickness: 1 mm, matrix: 512x512, FOV: 256x256 mm, slice no. 312, whole brain coverage, flip angle: 12°) and T2*-weighted BOLD EPI images (TR: 2500 ms, TE: 27 ms, 44x3mm axial slices providing whole-brain coverage, FOV: 288x288mm; matrix: 96x96, flip-angle: 81°) were acquired on a 3T GE MR750W Discovery scanner (GE, Milwaukee, USA). 270 volumes were acquired during the task fMRI protocol, which took approximately 12 minutes. Stimuli were displayed on a screen in the scanner room via a video projector. Participants saw the screen through a mirror applied to the head coil frame. Participants also underwent a resting state scan on a separate occasion with the same parameters as the task fMRI, except 240 volumes (10 minutes) were acquired. Participants were asked to lie motionless with their eyes open and remain awake during the scan. Resting-state and task fMRI scans were conducted on two separate occasions for all participants, with a difference of 1 to 3 weeks, at the same time of day.

1.3 PRE-PROCESSING

Pre-processing steps were performed via FEAT 6.0 as contained in the FMRIB Software Library (FSL (Smith et al. 2004)) and were the same for resting state and task fMRI scans to ensure comparability. The first 5 volumes were discarded to avoid saturation effects. Motion correction was applied using a rigid body (6 DOF) registration to the middle volume with MCFLIRT. Non-brain tissue was removed from the images via FSL's Brain Extraction Tool (Smith 2002). After a spatial smoothing step with a 6 mm FWHM Gaussian kernel, ICA-AROMA was used to identify and remove motion artifacts (Pruim et al. 2015). The denoised data additionally underwent nuisance regression to remove signal from the white matter and cerebrospinal fluid, and high pass temporal filtering with a 0.01 Hz cut-off. Resulting volumes were normalised to the standard 2mm MNI-space using a two-stage boundary-based registration process as implemented in FSL.

1.4 MULTIVARIATE ANALYSIS OF TASK-RELATED ACTIVATION

We performed a multivariate analysis of the activation maps using tensorial independent component analysis (TICA (Beckmann & Smith 2005; Tamás Kincses et al. 2008)). TICA performs a trilinear decomposition of the data into independent component matrices, which describe spatial, temporal and subject-dependent dimensions as per the following equation:

$$X_{ijk} = \sum_r A_{ir} B_{jr} C_{kr} + \epsilon_{ijk}, r=1\dots R$$

Here, X_{ijk} denotes the data of subject k at voxel location j and time point i . The matrices $A = [a_{ir}]$, $B = [b_{jr}]$ and $C = [c_{kr}]$ each contain R one-dimensional vectors which, for each estimated process r , characterize the temporal, spatial and subject-dependent signal variations, and ϵ is the confounding Gaussian noise. This trilinear combination is optimized via a least-squares approach so that different modes are maximally non-Gaussian. MELODIC thresholds spatial maps via an alternative hypothesis test based on fitting a Gaussian-Gamma mixture model to the distribution of voxel intensities within spatial maps and a posterior probability threshold of $p > 0.5$. The number of independent components was determined automatically using the Laplace approximation to the posterior evidence of the model order. ICs were classified as signal or noise based on their spatiotemporal characteristics, adherence to the task design and uniform expression across the subject pool (no outliers in subject modes). The advantage of TICA to the conventional statistical parametric mapping approach is the increased sensitivity to task-related and background activity during the task that helps discern more subtle alterations, in addition to being more robust to noise arising from head motion (Tamás Kincses et al. 2008), a feature convenient in the current study population.

1.5 ANALYSIS OF CONNECTIVITY MODULATION

Independently from the multivariate analysis, a parcellation-based connectivity analysis was also performed to investigate how resting state connectivity is modulated during the task. The Schaefer-atlas was used to divide the cortex into 100 parcels (Schaefer et al. 2018). The inverse of the registration warp fields was used to project atlas ROIs from MNI space to the native space of individual participants for the pre-processed resting state and task fMRI scans. Time courses for each ROI were extracted as the mean of underlying voxel time courses. Then partial correlation matrices were calculated independently for the task and resting state data. A Gaussian-gamma mixture model was fit to the connectivity distribution of the resting state partial correlation matrices (Bielczyk et al. 2018). Employing the approach termed task potency, both resting state and task partial correlation matrices were re-normalised using the parameters of the resting state main Gaussian (connections deemed inactive) to allow valid comparison (Chauvin et al. 2019). Modulation of connectivity was calculated by subtracting the resting state (baseline) connection strength from task connection strength. Resulting matrices of connectivity modulation values were thresholded at $t = \pm 3.1$ to only include connections consistently influenced by the task in the HC group. The extent of modulation in the included connections was compared between groups using a GLM-based approach with a

non-parametric permutation test for statistical inference (Winkler et al. 2014). Age and biological sex were included in the model as nuisance regressors. Correction for multiple comparisons was performed by controlling the family-wise error rate. Relationship to clinical variables (UPDRSIII-motor, Hoehn-Yahr stage) was calculated as the partial Spearman's correlation coefficient, corrected for age and biological sex.

1.5.1 Tensorial independent component analysis

The TICA analysis extracted 50 independent components (IC), out of which the first 2 were task-relevant networks. The first and second IC explained 19.6% and 19.41% of the total variance, respectively. IC1 contained the bilateral frontal eye fields, inferior frontal gyri, intraparietal sulci, higher order visual cortices (V3-5), bilateral lingual gyri, thalami, striatum and superior colliculi which were correlated with the attention part of the task in both conditions (COPE(color): $z=20.28$, $p<0.001$; COPE(motion): $z=22.00$, $p<0.001$). Areas of IC1 which anticorrelated with the attention part of the task (and correlated with the recall part) included the primary visual cortices, parietal operculi, dorsal anterior cingulate cortex, anterior insulae, inferior parietal lobules, superior temporal gyri and the cerebellum. IC2 contained, to a lesser extent, the intraparietal sulci and frontal eye fields, and more prominently, the primary and higher-level visual cortices and bilateral thalami. IC1 subject scores were significantly higher in the healthy group ($p<0.027$), adjusted for age and biological sex.

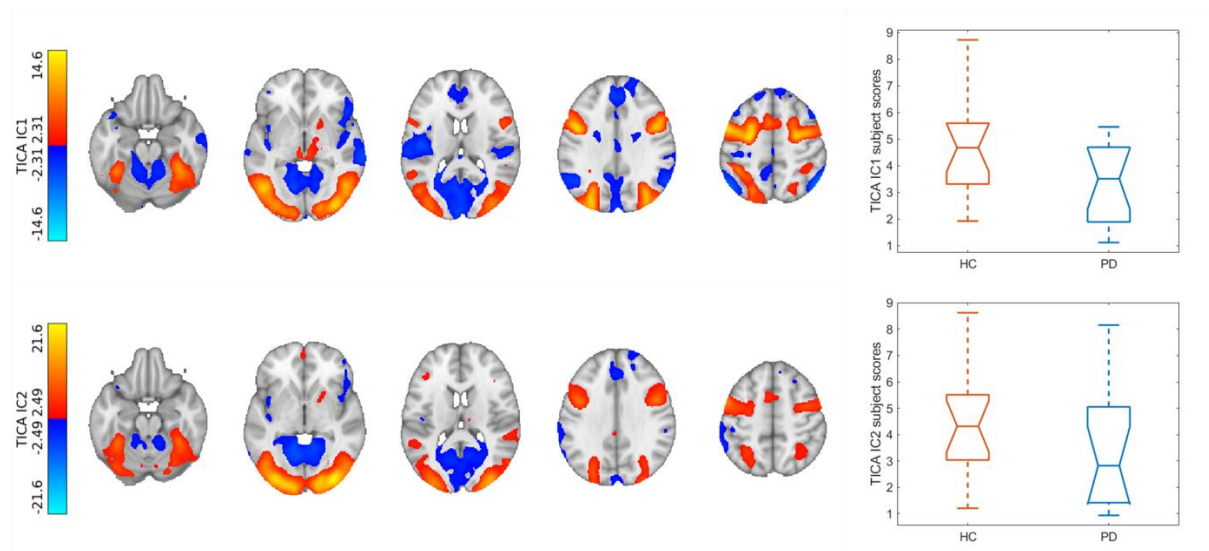


Figure 2. Results of the multivariate analysis. Spatial maps of task-relevant components were upsampled to 1 mm resolution and overlaid on the MNI152 1 mm template. Color bars denote Z-statistics. Box plots show group differences in subject modes of corresponding components. Abbreviations: TICA=tensorial independent component analysis; IC=independent component; HC=healthy control; PD=Parkinson's disease.

1.5.2 Connectivity modulation

Mainly nodes belonging to the visual frontoparietal, dorsal attention, ventral attention, default mode and somatomotor networks were consistently modulated during the task in the healthy cohort exemplified by a one-sample t-statistic of at least $t=3.1$ ($p<0.001$). The connection between the right primary visual cortex and parietooccipital cortex, as well as the connection between the right superior frontal gyrus and right opercular cortex was modulated to a significantly smaller degree in the PD cohort ($p<0.001$ and $p<0.013$, corrected for multiple comparisons). The connection between the right precuneus and the left ventromedial prefrontal cortex, as well as the connection between the left parietal operculum and lingual gyrus was modulated to a significantly higher degree in the PD cohort ($p<0.004$ and $p<0.011$, corrected for multiple comparisons).

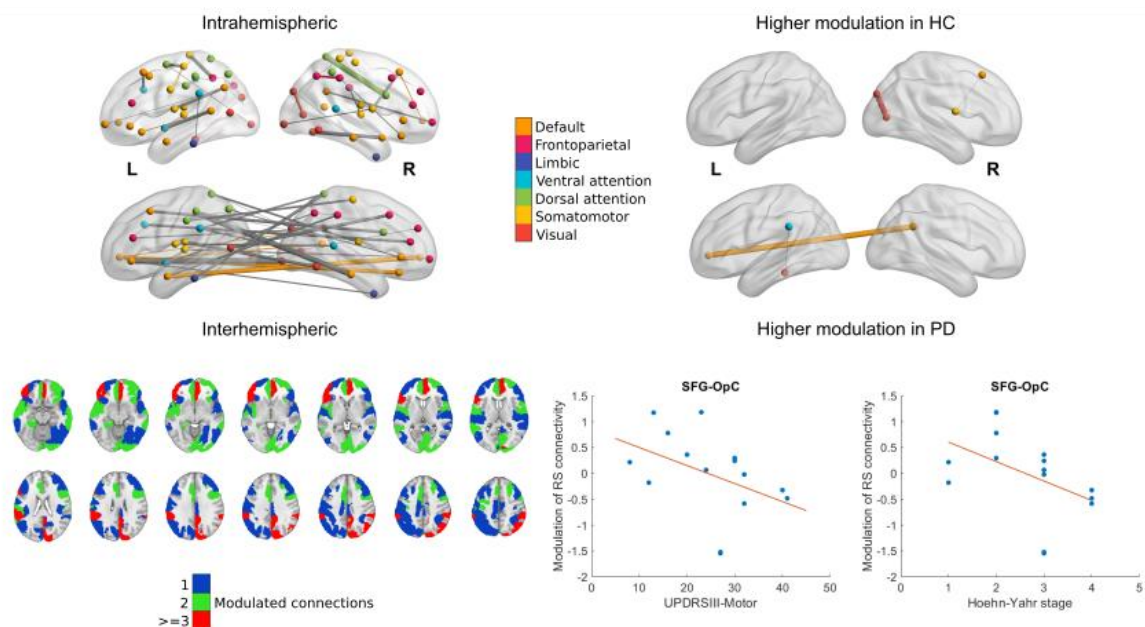


Figure 3. Modulation of cortical resting state functional connectivity during the task. 3D representations show relevant intra- and interhemispheric connections that were consistently modulated during the task in the healthy group (marked by a change with an effect size of at least $t=3.1$ in connectivity; left), or were modulated differently in the healthy and PD cohort (right). Nodes and within-network edges are color-coded according to their overlap with the 7-network parcellation in (Yeo et al. 2011); between-network edges are shown in gray. Axial slices show parcels from the Schaefer atlas with at least 1 connection modulated consistently group wise during the task. Parcel ROIs were overlaid on the MNI152 1 mm brain template and are shown in neurological orientation. Scatter plots show the statistically significant association between clinical characteristics and modulation of the superior frontal gyrus (SFG) – opercular cortex (OpC) connection in the PD cohort with a least-squares line superimposed.

1.5.3 Relationship to clinical characteristics

Subject scores of both IC1 and IC2 correlated significantly with UPDRSIII-motor scores and Hoehn-Yahr stages (IC1: $R = -0.72$, $p < 0.006$ and $R = -0.90$, $p < 0.001$; IC2: $R = -0.72$, $p < 0.006$ and $R = -0.89$, $p < 0.001$). Lower modulation of right superior frontal gyrus-right opercular cortex connectivity was associated with higher UPDRSIII-motor scores and Hoehn-Yahr stages ($R = -0.68$, $p < 0.01$; $R = -0.71$, $p < 0.007$).